# Tunneling of Cooper pairs across voltage-biased asymmetric single-Cooper-pair transistors

J. Leppäkangas,[1,*] E. Thuneberg,[1] R. Lindell,[2] and P. Hakonen[2]
[1]*Department of Physical Sciences, P.O.Box 3000, FI-90014 University of Oulu, Finland*
[2]*Low Temperature Laboratory, Helsinki University of Technology, FI-02015 TKK, Finland*
(Received 5 April 2006; revised manuscript received 5 June 2006; published 7 August 2006)

We analyze tunneling of Cooper pairs across voltage biased asymmetric single-Cooper-pair transistors. Also tunneling of Cooper pairs across two capacitively coupled Cooper-pair boxes is considered, when the capacitive coupling and Cooper pair tunneling are provided by a small Josephson junction between the islands. The theoretical analysis is done at subgap voltages, where the current-voltage characteristics depend strongly on the macroscopic eigenstates of the island(s) and their coupling to the dissipative environment. As the environment we use an impedance which satisfies $\mathrm{Re}[Z(\omega)] \ll R_Q$ and a few $LC$ oscillators in series with $Z(\omega)$. The numerically calculated $I$-$V$ curves are compared with experiments where the quantum states of mesoscopic SQUIDs are probed with inelastic Cooper pair tunneling. The main features of the observed $I$-$V$ data are reproduced. Especially, we find traces of band structure in the higher excited states of the Cooper-pair boxes as well as traces of multiphoton processes between two Cooper-pair boxes in the regime of large Josephson coupling $E_J \gg E_C$.

DOI: 10.1103/PhysRevB.74.054504 PACS number(s): 74.50.+r, 73.23.Hk, 74.78.Na

## I. INTRODUCTION

A voltage biased small Josephson junction (JJ) has been shown to be a good probe of mesoscopic physics. In recent years it has been used, for example, in the detection of resonances in the electromagnetic environment[1,2] and noise spectroscopy.[3,4] The theory of inelastic tunneling, known as the $P(E)$ theory, describes $I$-$V$ characteristics resulting from incoherent tunneling of Cooper pairs, or quasiparticles, across the small JJ and simultaneous energy exchange between the tunneling particle and its electromagnetic environment. The standard $P(E)$ theory cannot, however, be used in the case of a non-Gaussian or anharmonic environment. In this paper, a suitable model will be constructed to account for the anharmonic environment consisting of one or several JJs.

This paper gives a quantum description for a system which is designed to probe the excited states of a Cooper-pair box (CPB), or coupled boxes, by a small JJ. We model the quantum evolution of a voltage biased asymmetric single-Cooper-pair transistor (SCPT) or a circuit consisting of three JJs in series with a small middle JJ. The idea is, as in the $P(E)$ theory, that the small JJ is probing the eigenstates of the CPBs, which are then seen as current peaks at certain voltages. This is possible since under the voltage bias well above the supercurrent peak, but still at subgap region, the tunneling of a single Cooper pair across the small JJ is possible (nonvirtually) only if the environment is able to absorb the energy 2 eV released in the tunneling.

The environment of the small JJ consist of a CPB and a continuous spectrum of $LC$ oscillators describing dissipative quantum mechanics induced by high frequency resistive properties of the leads and possible spurious resonators in the transmission line or materials nearby the island. In resonant situations the dynamics involve both excitation and relaxation of the CPB eigenstates and one is, in principle, able to get information of both the energies as well as the relaxation times of the excited states.

Experimentally, the spectroscopy of the eigenstates using a small JJ as a probe have been done by Lindell *et al.* and the results are reported in Refs. 5–7. In this set of experiments, traces of excited states, their anharmonicity and expected band structure were found from the measured $I$-$V$ characteristics. However, several unexplained phenomena seen there were the main motivations for writing this more detailed description for the system. We show that indeed the main features of the $I$-$V$ data can be explained by the quantum mechanics of asymmetric SCPTs or coupled CPBs. The model explains, for example, the widening of the $I$-$V$ resonances as result of a band structure of (coupled) CPBs and nonconstant peak splitting in the experiment of Ref. 5 as a result of multiphoton transitions between eigenstates of two CPBs.

The paper is organized as follows. In Sec. II we build a theory describing inelastic tunneling across the small JJ when it has an anharmonic element, i.e., a CPB, in its environment. In Sec. III we discuss effects caused by slow relaxation and Sec. IV is devoted to a quantitative discussion of the $I$-$V$ characteristics in the case of a two CPB environment. Comparison between numerical calculations and experiments is presented in Sec. V and conclusions are given in Sec. VI.

## II. INCOHERENT TUNNELING OF COOPER PAIRS ACROSS ASYMMETRIC SCPT

We model an asymmetric single-Cooper-pair transistor by taking the Josephson coupling across the probe junction into account perturbatively. The treatment describes incoherent tunneling of Cooper pairs across the small JJ and simultaneous energy exchange between the tunneling Cooper pair, CPB and the dissipative environment. It is valid if the relaxation rates of the excited states are higher than the excitation rates induced by incoherent tunneling.

A voltage biased SCPT is shown in Fig. 1. We are interested in the case of strong asymmetry $E_{J1} \gg E_{J2}$. The charging energy of the island, defined as $E_C = e^2/2C_\Sigma$, where $C_\Sigma = C_0 + C_1 + C_2$, can, however, have an arbitrary value. Disregarding the Cooper pair and quasiparticle tunneling across the probe (the former is taken into account as a perturbation),

 

the Hamiltonian of the environment of the probe can be written formally as

$$H_{\mathrm{env}} = H_{\mathrm{CPB}} + H_{\mathrm{EE}} + H_{\mathrm{int}}, \tag{1}$$

where the CPB Hamiltonian is[8,9]

$$H_{\mathrm{CPB}} = \frac{(Q+Q_0)^2}{2C_\Sigma} - E_{J1}\cos(\varphi_1), \tag{2}$$

and $Q_0 = C_0 U - (C_2 + C_0/2)V$ is the quasicharge, $Q$ the island charge, a conjugated variable to the phase difference $\varphi_1$. The Hamiltonian $H_{\mathrm{EE}}$ models dissipative electromagnetic environment and possible spurious fluctuators in the system. Its characteristics are fully described by an impedance $Z(\omega)$, so formally it consist of an infinite number of harmonic oscillators. The interaction term $H_{\mathrm{int}}$ describes linear coupling between the CPB and the electromagnetic environment leading to dissipative quantum mechanics.[10]

To account for the anharmonicity and the band structure of the CPB, we will proceed slightly differently than is done in the $P(E)$ theory. The idea is to take the anharmonic parts into account separately. This is possible in the limit $\mathrm{Re}[Z(\omega)] \ll R_Q$, where the interaction between the CPB and the dissipative environment is weak and one can use the Born-Markov approximation when describing the evolution of the CPB under the Hamiltonian (1). In this limit the effect of the operator $H_{\mathrm{EE}} + H_{\mathrm{int}}$ for the CPB can be described by a transformation $V \to V + V_f$ in Eq. (2), where $V_f$ describes fluctuations from the average value $V$.[11,12] Therefore one can use an effective Hamiltonian for the CPB

$$H_{\mathrm{BM}} = H_{\mathrm{CPB}} - Q_{\mathrm{int}} V_f, \tag{3}$$

where $Q_{\mathrm{int}} = C_2 Q / C_\Sigma$ (we have assumed that $C_0 \ll C_\Sigma$). The autocorrelation function of the fluctuating voltage is related to the dissipative properties of the impedance $Z(\omega)$ via the quantum fluctuation-dissipation theorem

$$\langle V_f(t) V_f(0)\rangle_\omega = \int_{-\infty}^{\infty} dt e^{i\omega t} \langle V_f(t) V_f(0)\rangle = 2\,\mathrm{Re}[Z(\omega)] \frac{\hbar\omega}{1-\exp(-\hbar\omega/k_B T)}. \tag{4}$$

Since fluctuations are only a small perturbation to the CPB, their effect is to induce transitions between the unperturbed states, i.e., the eigenstates of the CPB. The transition rate between the eigenstates $|i\rangle$ and $|f\rangle$ is obtained by the golden rule calculation

$$\gamma_{f\leftarrow i} = \frac{2\,\mathrm{Re}[Z(\omega)]}{\hbar^2} |\langle f|Q_{\mathrm{int}}|i\rangle|^2 \frac{E_{if}}{1-\exp(-E_{if}/k_B T)}, \tag{5}$$

where $E_{if} = E_i - E_f = \hbar\omega$ is the difference between the corresponding eigenenergies.

We proceed by noting that the rates (5) define the lifetimes, and therefore also the linewidths, of the energy levels in the Cooper-pair box. The full width at half maximum (FWHM) $\Delta_\alpha$ of the state $|\alpha\rangle$ is then

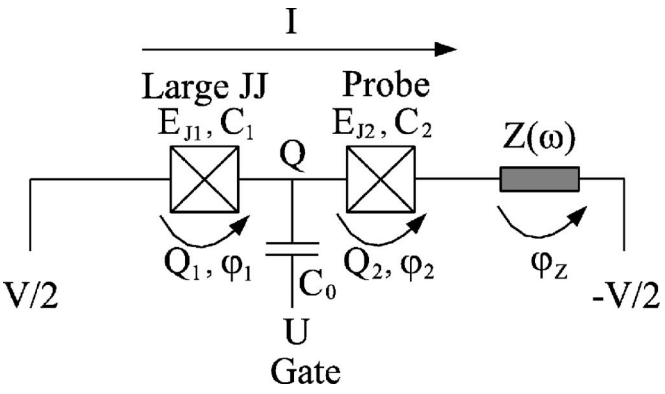


FIG. 1. A voltage biased SCPT. We study the case $E_{J1} \gg E_{J2}$ and the smaller JJ is called the probe. The superconducting leads (and the spurious environment of the island) are modeled through an impedance $Z(\omega)$.

$$\Delta_\alpha = \hbar \sum_f \gamma_{f\leftarrow\alpha}, \tag{6}$$

and the density of the excited states broadens from the sum of delta-functions to sum of Lorentzians, i.e., the density of states changes as

$$\sum_\alpha \delta(E - E_\alpha) \to \sum_\alpha \frac{2}{\pi} \frac{\Delta_\alpha}{4(E_\alpha - E)^2 + \Delta_\alpha^2}. \tag{7}$$

Finally, we include the Josephson coupling $E_{J2}\cos(\varphi_2)$ describing tunneling of Cooper pairs across the probe junction and simultaneous excitations of its environment as (another) perturbation. Using $\varphi_\Sigma = \varphi_1 + \varphi_2 + \varphi_Z = 2eVt/\hbar$, where $\varphi_Z$ is the phase difference across the impedance, one finds the time dependent perturbations for the positive and negative direction tunneling $M_\pm = E_{J2}\exp[\pm i(\varphi_1 + \varphi_Z - 2eVt/\hbar)]/2$.

For $\mathrm{Re}[Z(\omega)] \ll R_Q$, the transition rates between the eigenstates of $H_{\mathrm{env}}$ due to perturbations $M_\pm$ are effectively described by transition rates between the states $|\alpha\rangle|\mathrm{EE}\rangle$, which consist of two independent parts: *broadened* CPB states $|\alpha\rangle$ and the eigenstates $|\mathrm{EE}\rangle$ of the Hamiltonian $H_{\mathrm{EE}}$. The operator $\exp(i\varphi_1)$ acts to the $|\alpha\rangle$ states and $\exp(i\varphi_Z)$ to the $|\mathrm{EE}\rangle$ states. Therefore, the *LC* environment can be traced out similarly as in the $P(E)$ theory and the golden rule transition rates between the CPB states $|i\rangle$ and $|f\rangle$ become then

$$\Gamma^{\pm}_{f\leftarrow i} = \frac{E_{J2}^2}{\hbar} \int_{-\infty}^{+\infty} dE' P(\pm 2\ \mathrm{eV} - E') |\langle f|e^{\pm i\varphi_1}|i\rangle|^2 \times \frac{\Delta_i + \Delta_f}{4(E_f - E_0 - E')^2 + (\Delta_i + \Delta_f)^2}, \tag{8}$$

where the $P(E)$ function is the same as for a system consisting of a probe junction with a capacitance $C_{12} = (1/C_1 + 1/C_2)^{-1}$ in series with the impedance $Z(\omega)$. If $Z(\omega)$ is a constant $R(\ll R_Q)$, the main contribution of the $P(E)$ function becomes from low energies where it is approximately a Lorentzian with a linewidth $\Delta_{\mathrm{env}} = 4\pi k_B T R/R_Q$ centered at $E=0$ [2]. Therefore it convolutes the original transition rates (8) to

$$\Gamma^{\pm}_{f\leftarrow i} = \frac{E_{J2}^2}{\hbar}|\langle f|e^{\pm i\varphi_1}i|\rangle|^2 \frac{\Delta_{if}^{\text{total}}}{4(E_f - E_i \mp 2\ \text{eV})^2 + (\Delta_{if}^{\text{total}})^2}, \quad (9)$$

where $\Delta_{if}^{\text{total}} = \Delta_i + \Delta_f + \Delta_{\text{env}}$. We see that there are two sources of broadening of the resonances: widening due to finite lifetimes of the CPB eigenstates ($\Delta_\alpha$'s) and widening due to low frequency fluctuations of the $LC$ environment ($\Delta_{\text{env}}$). The separation of the CPB and its environment holds also for the case where the environment has several modes which are nondegenerate with the CPB eigenstates. The degeneration, or almost degeneration, would lead to similar splitting of the states as described in Sec. IV.

During each transition there is a transfer of $2e$ of charge across the probe. The net current across the system is therefore

$$I = 2e\sum_{fi} P_i(\Gamma^{+}_{f\leftarrow i} - \Gamma^{-}_{f\leftarrow i}), \quad (10)$$

where the probabilities $P_i$ for occupancies of the CPB eigenstates are given by the canonical equilibrium distribution. If $k_B T \ll E_1 - E_0$ and $Z(\omega) = R$ then

$$I(V) = 2e\sum_f \Gamma^{+}_{f\leftarrow 0} = \sum_f \frac{2eE_{J2}^2}{\hbar}|\langle f|e^{i\varphi_1}|0\rangle|^2 \times \frac{\Delta_f^{\text{total}}}{4(E_f - E_0 - 2eV)^2 + (\Delta_f^{\text{total}})^2}. \quad (11)$$

One sees that $I$-$V$ peaks can be identified with energy levels of the environment,[2,13] which in this case is the Cooper-pair box.

We have verified that the $I$-$V$ characteristics obtained from Eq. (11) reduce to the ones obtained from the $P(E)$ theory, if the larger JJ is described as an $LC$ oscillator. However, Eq. (11) is also valid for the JJ environment with evident anharmonicity or band structure, and therefore is not limited to the harmonic approximation.

## III. EFFECTS DUE TO SLOW RELAXATION

For the expression (9) to hold, it is vital that the system relaxes rapidly to the ground state, since the golden rule calculation is justified only if the excitation rates of the CPB eigenstates, induced by the probe, are smaller than the relaxation times, caused by the CPB's coupling to the dissipative environment. The irreversible interaction with the dissipative environment has to "cut" the evolution to the excited state quickly, otherwise the tunneling across the probe would turn from incoherent to coherent. On the other hand, in the opposite case of very slow relaxation, one would obtain Rabi oscillations between the CPB eigenstates $|0\rangle$ and $|\alpha\rangle$ when initially starting from the state $|0\rangle$ with $2\ \text{eV} = E_\alpha - E_0$. This limit can also be analyzed in the Born-Markov approximation,[14] but generally the problem needs an analysis of the time evolution of the whole density matrix and Markovian approximation cannot be used.[15]

To obtain approximative results in all regions, we use the model derived in Sec. II with modified probabilities for occupations. We redefine the diagonal elements of the density matrix by the ones obtained from the equilibrium master equation

$$\sum_{f\neq i}[P_f(\Gamma_{i\leftarrow f} + \gamma_{i\leftarrow f}) - P_i(\Gamma_{f\leftarrow i} + \gamma_{f\leftarrow i})] = 0, \quad (12)$$

for each $i$. The $\gamma$'s are the relaxation rates caused by the fluctuating voltage across the CPB, Eq. (5), whereas the $\Gamma$'s are the rates induced by Cooper pair tunneling across the probe, Eq. (9). The method assumes that all the sequential transitions are independent of each other, which is not always true. However, the method reduces to the one considered in Sec. II when the relaxation dominates the excitation and, according to our numerical calculations, gives similar results for the first order tunneling processes (single Cooper pair tunnels across the probe with simultaneous excitation of the CPB) even in the regime of very slow relaxation, as long as the SCPT is highly asymmetric. Therefore it is safe to assume that the first order processes are well approximated by Eq. (10) with the equilibrium probabilities obtained from Eqs. (12). Also, there is no experimental evidence of higher order resonances, which might be due to their weak nature to be washed out by the so-called Zeno effect.[15]

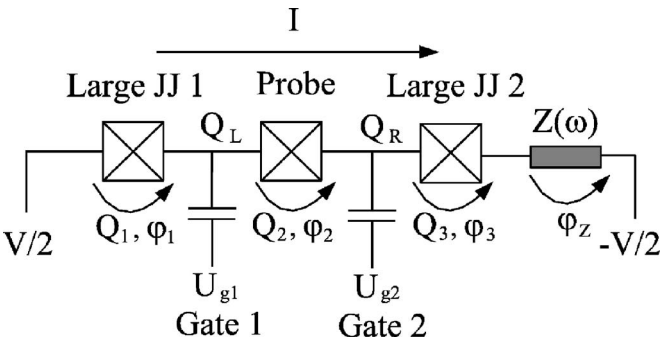


FIG. 2. Three Josephson junctions in series with the voltage source. One of the large JJs could as well as be an $LC$ oscillator, modeling the effect of a spurious resonance.

## IV. TWO CAPACITIVELY COUPLED CPBS

To generalize the treatment of the preceding sections, we do a perturbative treatment for three JJs in series, where the middle one acts as a probe. The configuration can be seen to consist of two capacitively coupled Cooper pair boxes,[16] where the capacitive coupling is in parallel with a small tunneling element. Since we use similar models for analyzing the experiments in Sec. V, we concentrate on the characteristics of this model a bit deeper. We also note that one of the larger JJ's could as well be an $LC$ oscillator describing spurious resonance at frequency $\omega_p = 1/\sqrt{LC}$ in the environment. If the energy quantum $\hbar\omega_p$ is almost the same as any excitation energy $E_n - E_m$ between two relevant eigenstates of the CPB, or the state is long living, it cannot be modelled by the $P(E)$ function in Eq. (8), but the following treatment is valid.

The system in consideration consists of three JJs in series connection with the voltage source and the smallest junction is in the middle, Fig. 2. Following the steps done in Sec. II,

we first neglect the Josephson coupling energy of the probe and write down the Hamiltonian of two capacitively coupled Cooper pair boxes

$$H_{2\mathrm{CPB}} = \frac{(Q_L+Q_0)^2}{2C_L} + \frac{(Q_R+Q_0')^2}{2C_R} - E_{J1}\cos(\varphi_1) - E_{J3}\cos(\varphi_3) + \frac{C_{123}Q_LQ_R}{C_1C_3}, \tag{13}$$

where $\varphi_1$ and $Q_L$ are conjugated variables and similarly for $\varphi_3$ and $Q_R$. The capacitances of the islands are (assuming that $C_{gi} \ll C_i$, where $C_{gi}$ is the capacitance of the gate $i$) $C_L = C_1 + C_{23}$, where $C_{23} = (1/C_2 + 1/C_3)^{-1}$, $C_R = C_3 + C_{12}$, and $C_{123} = (1/C_1 + 1/C_2 + 1/C_3)^{-1}$. The quasicharges become then $Q_0 \approx C_{g1}U_{g1} + C_{g2}U_{g2}C_2/C_R - C_2V$ and $Q_0' \approx -C_{g2}U_{g2} - C_{g1}U_{g1}C_2/C_L - C_2V$. One sees that the Hamiltonian consist of two CPB Hamiltonians, which are then coupled by the last term in Eq. (13). Similarly as in Sec. II, we first calculate the linewidths of the eigenstates of the coupled system (but now $Q_{\mathrm{int}} = Q_LC_2/C_L + Q_RC_2/C_R$), then use the fact that the phase difference $\varphi_\Sigma$ is a classical variable and take the tunneling across the probe into account perturbatively by considering the broadened states of the coupled CPBs and the environmental states separately. The current is obtained from Eq. (10), similarly as before.

The behavior of the eigenstates and energies of the Hamiltonian (13) can be analyzed analytically in the limit $E_{J1}$, $E_{J3} \gg e^2/2C_L, e^2/2C_R$. For simplicity let us assume that $E_{J1} = E_{J3} = E_J$ and $C_L = C_R \approx C_1 = C_3 = C$. Two "splitting" effects contribute to the final energy level structure of the coupled CPBs. First, in the harmonic approximation of Eq. (13) the CPB:s behave as *LC* oscillators. The degeneracy of the identical *LC* oscillators is removed by the interaction term $C_{123}Q_LQ_R/C_1C_3 \approx C_2Q_LQ_R/C^2$ (presuming that $C_2 \ll C$), and diagonalizing the quadratic Hamiltonian one sees that the system behaves as it would consist of two independent oscillators with the original inductances but with capacitances $\tilde{C}_\pm = C^2/(C \pm C_2)$. For small $C_2/C$ this leads to mode frequencies $\omega_p \pm \omega_p C_2/2C$. Secondly, if one takes into account the first nonharmonic terms $-E_J\varphi_i^4/4!$ in the Hamiltonian (13) and sets $C_2Q_LQ_R/C^2 = 0$, one obtains also energy level splitting effects due to combined energy levels of two anharmonic oscillators. The energy levels of single CPBs become $E_1 = \hbar\omega_p - E_C$, $E_2 = 2\hbar\omega_p - 3E_C$, $E_3 = 3\hbar\omega_p - 6E_C, \ldots$. New levels appear due to simultaneous excited states of the boxes

$$|2^*\rangle = |1\rangle|1\rangle, \tag{14}$$

$$|3^*\rangle = \frac{1}{\sqrt{2}}(|1\rangle|2\rangle + |2\rangle|1\rangle) \tag{15}$$

with the corresponding eigenenergies $E_{2^*} = 2\hbar\omega_p - 2E_C$ and $E_{3^*} = 3\hbar\omega_p - 4E_C$. The energy level $2\hbar\omega_p$ therefore "splits" into two nearby energy levels $E_2$ and $E_{2^*}$.

When both of the above effects are included, more mixing of the states is obtained. The $n$th excited state splits into $n+1$ states and, for example, the state $|1\rangle$ splits into states (using the first order perturbation theory)

$$|1s\rangle = \frac{1}{\sqrt{2}}(|1\rangle|0\rangle + |0\rangle|1\rangle), \tag{16}$$

$$|1a\rangle = \frac{1}{\sqrt{2}}(|1\rangle|0\rangle - |0\rangle|1\rangle) \tag{17}$$

with the eigenenergies $E_{1s} = \hbar\omega_p - z - E_C$ and $E_{1a} = \hbar\omega_p + z - E_C$, where $z = C_2\hbar\omega_p/2C$. Similarly for the state $|2\rangle$

$$|2s\rangle = c_1(|2\rangle|0\rangle + |0\rangle|2\rangle + c^+|1\rangle|1\rangle), \tag{18}$$

$$|2a\rangle = \frac{1}{\sqrt{2}}(|2\rangle|0\rangle - |0\rangle|2\rangle), \tag{19}$$

$$|2^*\rangle = c_2(|2\rangle|0\rangle + |0\rangle|2\rangle + c^-|1\rangle|1\rangle), \tag{20}$$

where $E_{2s} = 2\hbar\omega_p - 5E_C/2 - z'$, $E_{2a} = 2\hbar\omega_p - 3E_C$, $E_{2^*} = 2\hbar\omega_p - 5E_C/2 + z'$, $c^\pm = (-E_C/2 \pm z')/\sqrt{2}z$, $z' = \sqrt{E_C^2 + 16z^2}/2$ and $c_i$ are normalizing factors. These states give both behaviors discussed in the preceding paragraph as the limiting cases of $E_C \to 0$ and $z \to 0$, respectively. The states $|1a\rangle$ and $|2a\rangle$ do not lead to current peaks since they contain antisymmetric combination of the states and therefore the elements $|\langle f|\exp[\pm i(\varphi_L + \varphi_R)]|0\rangle|$ vanish. We still pick up the energies of the states $E_{3s} = 3\hbar\omega_p - 5E_C - z - \sqrt{E_C^2 + 4z^2 - 2E_Cz}$ and $E_{3^*} = 3\hbar\omega_p - 5E_C - z + \sqrt{E_C^2 + 4z^2 - 2E_Cz}$.

For higher anharmonicity ($E_J \sim E_C$), where the band structure will become evident for the eigenstates and the perturbative treatment of the cosine potential is no longer valid, we have to resort to numerical solution. We calculate the eigenstates by diagonalizing the Hamiltonian in a product basis of two noninteracting CPBs, for given values of gate voltages (quasicharges). The lowest eigenstates can be obtained quite accurately from an economical sized matrix equation, since the eigenstates are usually close to the states of this basis (due to small capacitive coupling), justifying also the "product state labeling" of the final states. After the Hamiltonian is diagonalized (and the transition rates have been calculated) one has to solve Eqs. (10) and (12) for each value of $V$ to obtain the $I$-$V$ characteristics for given $U_{gi}$.

In Sec. V B we model experiments using a similar circuit but including also two extra *LC* oscillators in series with the three JJ system. The previous $I$-$V$ characteristics of the coupled CPBs are still preserved but multiphoton transitions with the external *LC* oscillators are also obtained, which is the motivation for this procedure. In practice, the extra *LC* oscillators can be modelled as JJs and the Hamiltonian of the system can be written as

$$H = \sum_{k,l} \frac{1}{2}(C^{-1})_{kl}q_kq_l - \sum_i E_{Ji}\cos(\varphi_i), \tag{21}$$

where $q_k = Q_k - Q_{k+1}$, $Q_k$ is the charge gone through the $k$th JJ, a conjugate variable to $\varphi_i$, $C$ is a capacitance matrix.[1] This Hamiltonian fully determines the energy bands, i.e., the ranges where peaks can occur in $I$-$V$ characteristics. In order to determine further details such as the peak positions for given gate voltages, one has to complete the Hamiltonian with linear terms in charge. Such terms result from voltage

sources and can be deduced from single tunneling events.[1,18] However, it turns out that in the experiments to be analyzed, the quasicharge is averaged over all values and the resonance positions become immune to these terms.

The relaxation rates due to photon emission to the electromagnetic environment $Z(\omega)$ are also determined by linear terms, through the fluctuating operator $Q_{\rm int}V_f=\Sigma_i a_i Q_i V_f$. For the *LC* oscillators this relaxation channel does not lead to observed rates and must be enhanced by introducing resistors in parallel with $L$ and $C$. An analogous procedure is to take the coefficients $a_{LC}$ as fitting parameters and use the operator $\Sigma_i a_{LCi} Q_{LCi} V_{LCi}$ as a perturbation, where the fluctuations $V_{LCi}$ are uncorrelated but have the original properties. For the large JJs $a_i$'s are theoretically defined by the ratios $C_2/C_{L/R}$, as was seen in the beginning of this section. The ratios are locked when fitting the observed energy level structure of the coupled system. But in real systems the capacitive coupling of CPBs can be effectively reduced by decoherence effects, for example by thermal fluctuations or dissipation, leading to a decrease in the "observed" $C_2$. Also effects related to materials nearby the CPB islands seem to be able to increase relaxation.[17] Therefore in modeling the relaxation rates of coupled CPBs, one is forced to take the corresponding coefficients $a_i$ as independent fitting parameters.

## V. COMPARISON TO EXPERIMENTS

The *I-V* characteristics of similar systems as discussed above were measured experimentally by Lindell *et al.* and reported in Refs. 5–7. In these experiments, different kind of environments for the probe junction, consisting of one or several SQUIDs and two or four leads, were used under different magnetic fields and gate voltages. Using SQUIDs as the large JJs, the system could be studied *in situ* from the harmonic behavior ($E_{J1} \gg E_C$) to the region where the anharmonicity and band structure become crucial ($E_{J1} \sim E_C$), by applying magnetic flux to the SQUID loops. This property also helped in the analysis of the data, since resonances coming from the spurious environment did not react to the applied magnetic field, at least not in the same way as the resonances coming from the CPBs.

The probe junction current as a function of voltage and external flux is shown in Fig. 3 as a 2D-surface plot. The dominant current peaks show periodicity as a function of the flux $\Phi$ through the SQUID loop with the period of the flux quantum $\Phi_0=h/2e$. This clearly points that they are originating from the SQUIDs and allows the identification of the different SQUID excitation states from the more complicated *I-V* structure due to the rest of the electromagnetic environment. In addition to the periodic structures due to the SQUID environment, one can see additional states with longer and nonconstant periods. It is likely that these are due to large, additional, Josephson junctions that are created in the two-angle evaporation technique used to fabricate the sample. The patterns have the Fraunhofer/Airy behavior as expected for a large Josephson junction that is penetrated by a magnetic field.[18]

### A. The 1-SQUID experiment

We begin by studying the sample that has the configuration of the asymmetric SCPT (Fig. 1). The first thing in the fitting procedure is to identify which of the resonances in the *I-V* characteristics are coming from the CPB eigenstates, which from spurious fluctuators and which from simultaneous excitations of both. The *I-V* peaks in this "1-SQUID experiment" consist of a set of flux dependent double peaks and several static resonances, from which the most important is at $V_{LC} \approx 13\ \mu$V, i.e., $\omega_0/2\pi \approx 6.3$ GHz, see Fig. 4. Its second excited state is seen at $2V_{LC} \approx 26\ \mu$V (not shown in Fig. 4) and therefore it is not a two-state fluctuator. The resonance is important since it explains the double structure of the first two flux-dependent double peaks: the lower resonance of each double peak is due to tunneling of a Cooper pair across the probe and simultaneous excitation of the CPB and the higher resonance of each double peak is due to tunneling and simultaneous excitations of the CPB and the *LC* resonance (a multiphoton transition). Two observations support this idea. First, the peak splitting is constant as a function of $E_{J1}(\Phi) = E_{J1}\cos(\pi\Phi/\Phi_0)$ and this constant is the same for the first and the second double peaks and also equals $V_{LC}$, reflecting the same excitation energy difference $2eV_{LC}$, see Fig. 4. Secondly, when compared to the first peak of a double peak, the *relative* area of the second one is approximately the same for the first two double peaks, indicating a similar extra factor (matrix element) related to the latter resonance of a double peak. The theoretical model used in fitting is the same as in Sec. IV except that one of the JJs is replaced by an *LC* oscillator.

The third double peak is not, however, consistent with similar interpretation, since the peak splitting is smaller than the previous ones at $\Phi=0$ and increases with increasing $\Phi$. Also, the two resonances of the double peak have almost equal areas, but the multiphoton transition to the external *LC*

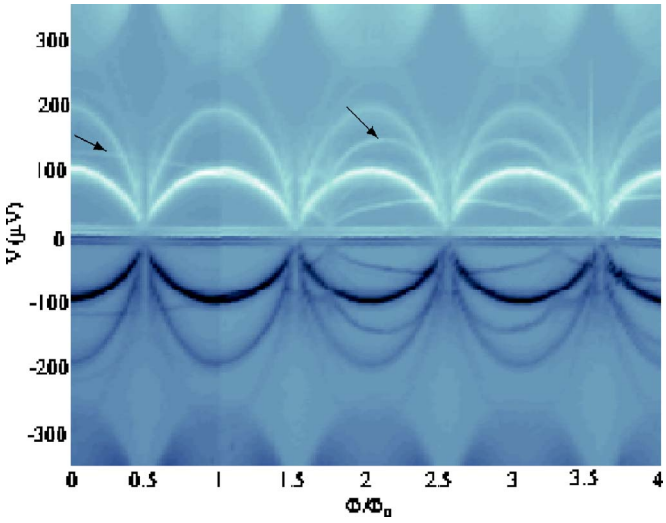


FIG. 3. (Color online) A 2D-surface plot of the measured probe junction current as a function of voltage and flux through the SQUID loop. The resonances originating from the SQUIDs show $\Phi_0$-periodicity. The figure also shows a resonance of Fraunhofer/Airy type with weaker dependence on $\Phi$ (pointed by the left arrow), and multiphoton transitions between the SQUID and the fluctuator behind this resonance (the right arrow). The *I-V* characteristics of this 4-SQUID sample are analyzed more quantitatively in Sec. V B.

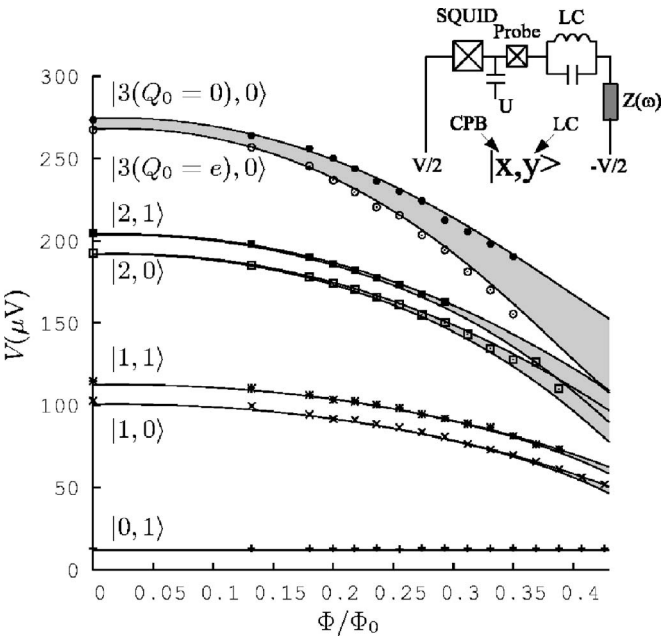


FIG. 4. The positions of the resonances in the 1-SQUID experiment (data points) compared with those resulting from the model of a SQUID and an *LC* oscillator in series with the probe junction (lines). The resonances have been labeled by the corresponding transitions behind them. For example, $|1,0\rangle$ means that the resonance occurs due the transition from the ground state to the product state, in which the CPB is in its first excited state and the *LC* oscillator stays in its ground state. The energy levels of the CPBs are actually bands (shaded), meaning that the levels are quasicharge $Q_0=C_0U-(C_2+C_0/2)V$ dependent. The resonances due to the band edges $Q_0=0$, $Q_0=e$ have been plotted explicitly. The parameters in the numerical modeling are summarized in Table I.

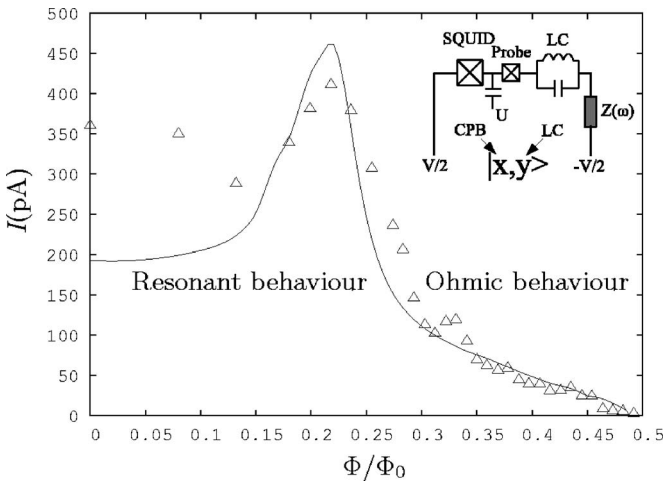


FIG. 5. The maximum current of the resonance $|1,0\rangle$ in the 1-SQUID experiment (triangles) compared with that resulting from the model of a SQUID and an *LC* oscillator in series with the probe junction. The *I-V* curves of the model were averaged over all values of the quasicharge. Different from Fig. 4, the *LC* oscillator ("*LC*2" in Table I) describes a small *I-V* peak seen at a voltage $\approx 90\ \mu$V (not shown in Fig. 4). In the region $\Phi > 0.3\Phi_0$ the state $|1,0\rangle$ suffers from a slow relaxation and the current is determined by the photon emission to the Ohmic low frequency environment. A resonance occurs nearby $\approx 0.2\Phi_0$ when the states $|1,0\rangle$ and $|0,1\rangle$ are coupled, the latter having a faster relaxation to its ground state. The current between $\Phi=0$ and $\Phi=0.1\Phi_0$ seems also to be enhanced, probably due to further entanglement with the environment. In the calculation of the relaxation rates we have used a perturbation $C_2Q_{\mathrm{SQUID}}V_f/(C_1+C_2)+0.13Q_{LC}V_{f'}$ (Sec. IV).

oscillator should have almost vanishing area and should not even be seen. The peak splitting can be explained by the band structure of the CPB's third excited state, assuming that the observed *I-V* curves are certain averages of the quasicharge-space and band edges are highlighted due to van Hove–like singularities. The observed splitting indeed follows the resonances obtained from band edges, as seen in Fig. 4. Still, the physical reason for the "escape" of the quasicharge is unknown. One possibility is a fluctuating background charge $Q_{00}$, which then mixes the effective quasicharge $Q_0+Q_{00}$. No gate dependence for the positions of the *I-V* peaks is seen in the experiments when $E_{J1} > E_c$, supporting the idea of the running polarization charge. It is, interestingly, returned in the limit $E_{J1} < E_c$ at higher voltages as charging effects, when the quasicharge dependence of the ground state energy becomes observable.

Indications of the band structure of $|2,0\rangle$ and even $|1,0\rangle$ excitations are seen in the experiment for $\Phi > 0.3\Phi_0$ and $\Phi > 0.4\Phi_0$, respectively, but instead of clear splitting the resonances widen and become fluctuating. This broadening is also expected theoretically, as shown in Fig. 4, and looks to be caused by random quasicharge fluctuations. Unfortunately the noise induced by the environment exceeds these current peaks for $\Phi > 0.35\Phi_0$ and therefore no clear evidence of these bands is obtained.

Finally, we note that the linewidths of the resonances are similar for the lowest resonances $\sim 8\ \mu$V, which can be fitted using the values $R_0=200\ \Omega$, $T=0.2$ K (leading to $\Delta_{\mathrm{env}}/2e \sim 3.5\ \mu$V) and the independently measured value $E_{J2}=8.5\ \mu$eV. This "effective" temperature is higher than the experimental value $\sim 0.1$ K. The model indicates that the lowest resonances are in the slow relaxation regime, which is consistent with the observation that the maximum current of the $|1.0\rangle$ resonance decreases when the magnetic flux is increased, see Fig. 5.

### B. The 4-SQUID experiment

The second sample to be studied consists of four leads, four SQUIDs and a probe junction, see left side of Fig. 6. Since the two SQUIDs on the same side of the probe behave as a SCPT and the phase difference $\theta$ across this component relaxes to the minimum energy value $\theta=0$ (its classical dynamics is highly damped and no bias is present), the two SQUIDs behave as a single JJ and one arrives at an equivalent circuit of two JJs and a probe in series connection; the model discussed in Sec. IV.

Also for this sample, the *I-V* characteristics consist of flux dependent double peaks and a few static resonances. The noise of the environment in the limit $E_{J1} \sim E_C$ is, however, much smaller than in the 1-SQUID sample, probably due to smaller $E_{J2}$ or better symmetry of the experiment. Again, the

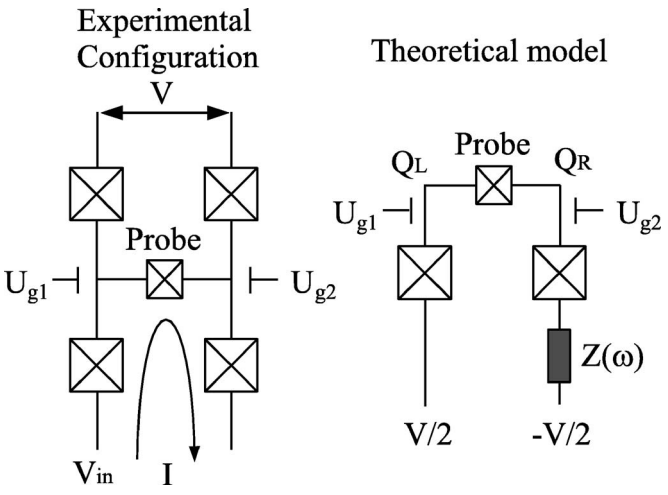


FIG. 6. Left: Schematic drawing of the 4-SQUID experiment. The SQUIDs are drawn as JJs. In this situation, the two SQUIDs (at the same side) behave as a single JJ, but with double the coupling energy $E_J$ and capacitance $C$ compared to the individual SQUIDs. Right: The resulting theoretical model of the system.

first static resonance is seen at $V_{LC} \approx 11\ \mu$V, i.e., $\omega_0/2\pi \approx 5.3$ GHz, see Fig. 7, and its second excited state is seen at $2V_{LC}$ (not shown in Fig. 7). We include also a resonance seen at $V_R \approx 123\ \mu$V to the model as another $LC$ oscillator. The first flux dependent double peak can again be explained a as a plain excitation of the CPB, and a multiexcitation of the CPB and the (smaller frequency) $LC$ oscillator. The second

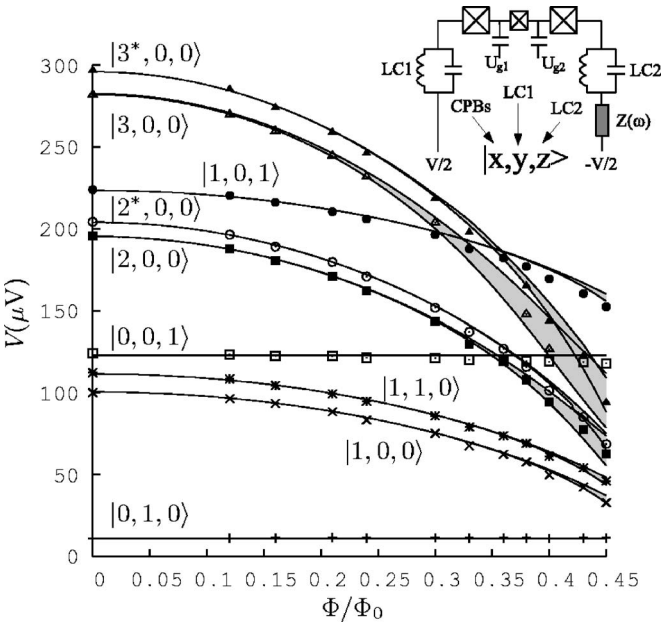


FIG. 7. The positions of the resonances in the 4-SQUID experiment (data points) compared with the edges of the energy bands (lines) and the band structure (shaded) calculated from the model of two SQUIDs and two $LC$ oscillators in series with the probe junction. The experimental data is based on $I$-$V$ curves of which two examples are shown in Fig. 8. Also shown is a schematic diagram of the model circuit and the code used for labelling the states. The parameters in the numerical model are summarized in Table I.

TABLE I. Parameter values used to fit the experimental $I$-$V$ curves. The values resulting from independent measurements(Ref. 5) are given in parentheses. We note that the experimental value for $E_{J1}$ in the 1-SQUID experiment, obtained via a normal state resistance measurement, is unreliable because it was obtained after the probe was accidentally broken. When modeling the 1-SQUID sample, we used an asymmetry factor $d=0.12$ for $E_{J1}$, i.e., the Josephson coupling energies of the two JJs inside a SQUID satisfy $|E_{JJ1}-E_{JJ2}|/E_{J1}=0.12$.

| Sample | $E_{J1}$ ($\mu$eV) | $E_{J2}$ ($\mu$eV) | $C_1$ (fF) | $C_2$ (fF) | $T$ (K) |
|---|---|---|---|---|---|
| 1-SQUID | 390 (188) | 8.5 (8.5) | 4.8 (5.7) | 0.5 (0.8) | 0.2(0.1) |
| 4-SQUID | 483 (544) | 3.6 (3.6) | 6.45 | 0.15 (0.5) | 0.2(0.1) |
| | $Z(0)(\Omega)$ | $L_1$ (nH) | $L_2$ (nH) | $C_{LC1}$ (fF) | $C_{LC2}$ (fF) |
| 1-SQUID | 200 | 3.1 | 0.13 | 240 | 100 |
| 4-SQUID | 100 | 3.8 | 0.3 | 240 | 24 |

double peak, however, is not consistent with this assumption since the peak splitting is much smaller than $V_{LC}$, 8.5 $\mu$V, and the relative areas of the peaks 1:0.4 differ essentially from the ones observed for the first double peak 1:0.13. Instead, a better explanation for the second double peak is the energy level structure of two coupled CPBs in the anharmonic region (Sec. IV); the peak splitting occurs due to resonances of the $|2,0,0\rangle$ and $|2^*,0,0\rangle$ excitations, and using the parameters given in Table I one obtains a peak splitting 8.5 $\mu$V and an area ratio 1:0.25. The resonances corresponding to the multiphoton transitions $|2,1,0\rangle$ and $|2^*,1,0\rangle$ are also seen as weak peaks in agreement with the model. The third double peak splitting is then automatically explained as excitations to the states $|3,0,0\rangle$ and $|3^*,0,0\rangle$, giving the peak splitting 13.2 $\mu$eV and area ratio 1:1. The experimental values are 15.0 $\mu$eV and 1:1. Note, that in this sample the band structure of the state $|3,0,0\rangle$ is neglible at $\Phi=0$, and therefore it does not explain the third double peak. The multiexcitation $|1,0,1\rangle$ is also seen in Figs. 3 and 7, justifying generally the multiphoton interpretation.

We conclude that the area ratio and the peak splitting of the first double peak can be fitted by changing the properties of the external $LC$ oscillator but at the same time the resonance at $V=V_{LC}$ has to be fitted also, whereas the other splittings and areas are determined by the charging energy $E_C$ of the island(s) and the capacitance of the probe junction $C_2$ (Sec. IV). Also adding a slight asymmetry between the two SQUIDs can "fine-tune" these values and we have used here a 1% difference. From Fig. 8 one can see that, not only the calculated positions of the resonance peaks, but also the corresponding areas are quite similar for the model and experiment for this choice of fitting parameters.

It is interesting to study the effect of band structure in this experiment. Again, a change in the gate voltage did not result in a change of the resonance positions, even in the region $E_{J1}-E_C$. Instead, the resonances originating from SQUIDs widened and changed from smooth Lorentzians to fluctuating lines. Therefore, we again assume that the mea-

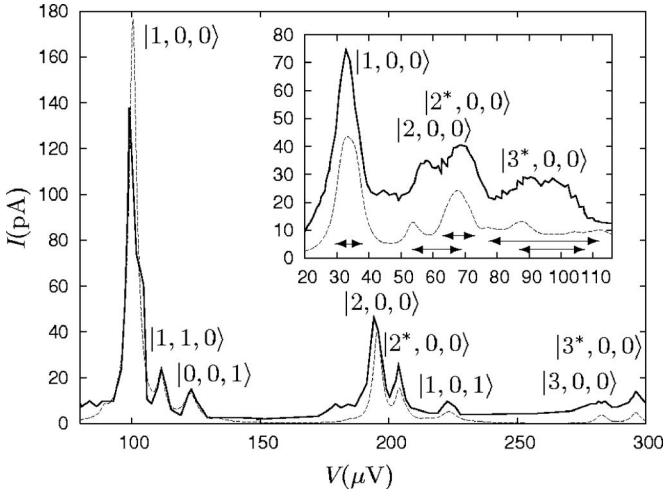


FIG. 8. The current across the 4-SQUID sample when $\Phi=0$ (main frame) and $\Phi=0.45\Phi_0$ (inset). The solid line is the experimental and the dashed line the theoretical *I-V* curve. For the theoretical fit we have averaged over all values of $Q_0$ and $Q_0'$ and the widths of the bands are indicated as arrows. In the inset one can see that the $|1,0,0\rangle$ resonance has widened and centers at $\sim 32$ $\mu$V. The $|2^*,0,0\rangle$ resonance lies almost at the same point as the upper edge of the $|2,0,0\rangle$ resonance, making the overall structure asymmetric. The $|3^*,0,0\rangle$ resonance lies between $\sim 88$ and $\sim 108$ $\mu$V, and the $|3,0,0\rangle$ resonance lies between $\sim 78$ and $\sim 112$ $\mu$V. In the calculation of the relaxation rates we have used $Q_{\rm int}=0.2(Q_1+Q_3+Q_{LC1}+Q_{LC2})$ (Sec. IV).

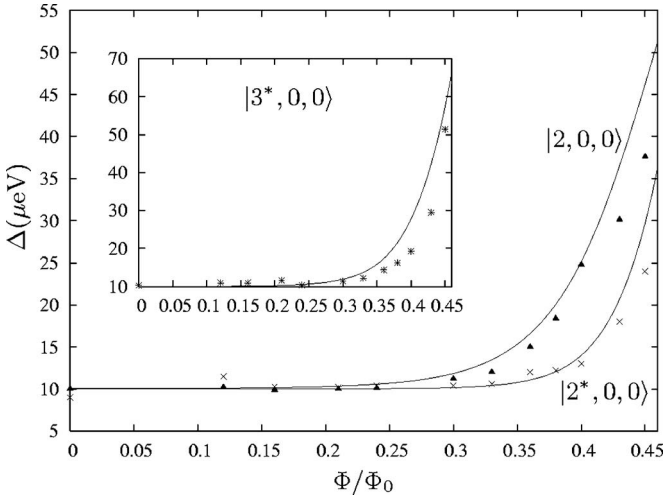


FIG. 9. Experimental linewidths (data points) compared with theoretical linewidths (lines) for three of the resonances as a function of the magnetic flux. The theoretical values are obtained by adding a constant term 10 $\mu$eV to the widths of the bands.

sured *I-V* curves are a result of some kind of averaging over the qu-sicharge space, which is now two dimensional because of two quasicharges $Q_0$ and $Q_0'$. The theoretical and experimental *I-V* curves are compared at $\Phi=0.45\Phi_0$ in the inset of Fig. 8. One can see that they compare fairly well, even though the peak heights for show little disagreement. In this sample the band structure does not lead to strong peak splitting in contrast to the 1-SQUID sample. The reason for this is that the van Hove singularities in two dimensional quasicharge space are weaker than in one dimension. This is not the case for single excitations $|1,0,0\rangle$, $|2,0,0\rangle$, and $|3,0,0\rangle$, and indeed the band edges of the latter two are seen as separate peaks in the theoretical *I-V* curve. We have used uniform quasicharge distribution, which is the simplest guess as the physics of the average processing are unknown.

The experimental and theoretical peak broadening are compared in Fig. 9 for three of the transitions. The theoretical width is obtained by summing up the peak width at $\Phi=0$ and the increase due to broadening of the bands. The peak width at $\Phi=0$ is $\sim 10$ $\mu$eV and the best fit is obtained by using $R_0=100$ $\Omega$, $T=0.2$ K, and the independently measured value $E_{J2}=3.6$ $\mu$eV. The experimental temperature is $T\sim 0.1$ K. There is a good agreement between the theory and experiment. For example, the $|2,0,0\rangle$ resonance broadens faster than the $|2^*,0,0\rangle$ resonance which is consistent with the theoretical model. The width of the $|3,0,0\rangle$ resonance is not analyzed since it rapidly becomes unobservable due to strong broadening.

## VI. CONCLUSION

We have carried out a theoretical study of Cooper pair tunneling across a voltage biased asymmetric SCPT and a system consisting of three JJs in series, where the middle one acts as a probe, and applied the models in analyzing the experimental findings of Ref. 5. The treatment of the problem was done in the weak coupling regime, where the Cooper pairs tunnel incoherently across the probe, and was based on the idea of extending the well known $P(E)$ theory into the regime where the anharmonicity and band structure are taken into account. We pointed out, that the nature of the tunneling across the probe turns from incoherent to coherent when the golden rule tunneling times exceed the relaxation times induced by the dissipative environment. Furthermore, we discussed that a simple master equation correction to the population of the eigenstates in the incoherent calculation leads to a good approximation for the current for arbitrary values of the voltage and for different flux values.

In the last part of this paper we showed that a detailed theoretical understanding of experimental data can be achieved. In particular, the multiphoton processes between different mesoscopic elements and spurious *LC* resonators as well as the band structure of the Josephson junction can be probed by a small Josephson junction coupled to SQUID(s). Especially, the detection of energy bands of higher excited states is confirmed by the fact that the observed widening of the resonances was in good accordance with the linewidths obtained from the model.

## ACKNOWLEDGMENTS

This work was financially supported by the National Graduate School in Material Physics, Finnish Academy of Science and Letters (Vilho, Yrjö and Kalle Väisälä Foundation) and the Academy of Finland (National Center of Excellence Programme).

*Electronic address: juha.leppakangas@oulu.fi

[1] G.-L. Ingold and Y. V. Nazarov, *Single Charge Tunneling*, edited by H. Grabert and M. H. Devoret (Plenum, New York, 1992).
[2] G. L. Ingold, H. Grabert, and U. Eberhardt, Phys. Rev. B **50**, 395 (1994).
[3] E. B. Sonin, Phys. Rev. B **70**, 140506(R) (2004).
[4] R. K. Lindell, J. Delahaye, M. A. Sillanpää, T. T. Heikkilä, E. B. Sonin, and P. J. Hakonen, Phys. Rev. Lett. **93**, 197002 (2004).
[5] R. Lindell, J. Penttilä, M. Sillanpää, and P. Hakonen, Phys. Rev. B **68**, 052506 (2003).
[6] R. Lindell, J. Penttilä, M. Paalanen, and P. Hakonen, Physica E (Amsterdam) **18**, 13 (2003).
[7] R. Lindell, Ph.D. thesis, Helsinki University of Technology, Helsinki 2005.
[8] D. V. Averin, A. B. Zorin, and K. K. Likharev, Sov. Phys. JETP **61**, 407 (1985).
[9] K. K. Likharev and A. B. Zorin, J. Low Temp. Phys. **59**, 347 (1985).
[10] U. Weiss, *Quantum Dissipative Systems*, 2nd ed. (World Scientific, Singapore, 1999).
[11] A. Maassen van den Brink, A. A. Odintsov, P. A. Bobbert, and G. Schön, Z. Phys. B: Condens. Matter **85**, 459 (1991).
[12] A. Maassen van den Brink, G. Schön, and L. J. Geerligs, Phys. Rev. Lett. **67**, 3030 (1991).
[13] T. Holst, D. Esteve, C. Urbina, and M. H. Devoret, Phys. Rev. Lett. **73**, 3455 (1994).
[14] J. Leppäkangas and E. Thuneberg (unpublished).
[15] A. Shnirman and Yu. Makhlin, JETP Lett. **78**, 447 (2003).
[16] Yu. A. Pashkin, T. Yamamoto, O. Astafiev, Y. Nakamura, D. V. Averin, and J. S. Tsai, Nature (London) **421**, 823 (2003).
[17] O. Astafiev, Yu. A. Pashkin, Y. Nakamura, T. Yamamoto, and J. S. Tsai, Phys. Rev. Lett. **93**, 267007 (2004).
[18] M. Tinkham, *Introduction to Superconductivity*, 2nd ed. (McGraw-Hill, New York, 1996).